Table 2. Area Under the ROC Curves, Sensitivity, Specificity, and Negative as Well as Positive Predictive Values of Nonvirological Responses

Variables	AUC	95% CI	Cutoff	Sensitivity	Specificity	NPV	PPV
RIG-I (copies/int. control)	0.712	0.584-0.840	0.573	0.679	0.733	0.830	0.543
ISG15 (copies/int. control)	0.782	0.666-0.899	0.347	0.714	0.833	0.862	0.667
RIG-I/IPS-1 (copies/int. control)	0.732	0.611-0.852	0.651	0.679	0.750	0.833	0.559
IL28B genotype	0.662	0.537-0.787	TG*/CT†	0.607	0.717	0.796	0.500

AUC, area under the curve; NPV, negative predictive value; PPV, positive predictive value.
*Genotype at rs8099917.
†Genotype at rs12979860.

associated with NVR (Table 3). Among these, multivariate analysis identified old age, HCV core double mutant, and higher hepatic expressions of *RIG-I* and *ISG15* as factors independently associated with NVR (Table 3).

IPS-1 and RIG-I Protein Expression in the Liver. Western blotting revealed that full-length and cleaved IPS-1 were variably present in all the samples from CH-C patients (Fig. 5A). Similar to mRNA

Table 3. Factors Associated with Nonvirological Response

Factors	Univariate Analysis		Multivariate Analysis*	
	Risk Ratio (95% CI)	P-value	Risk Ratio (95% CI)	P-value
Age (by every 10 year)	1.84 (1.10-3.14)	0.027	3.76 (1.19-11.7)	0.023
Sex				
Male	1			
Female	1.62 (0.59-4.42)	0.350		
BMI (by every 5 kg/m²)	0.87 (0.46-1.65)	0.672		
Fibrosis stage				
F1/F2	1			
F3/F4	1.82 (0.69-4.85)	0.228		
Degree of steatosis				
<10%	1			
≥10%	1.46 (0.43-5.03)	0.544		
Albumin (by every 1 g/dL)	0.41 (0.11-1.56)	0.190		
AST (by every 40 IU/L)	0.89 (0.53-1.56)	0.681		
ALT (by every 40 IU/L)	0.85 (0.57-1.32)	0.481		
γ-GTP (by every 40 IU/L)	1.32 (0.82-2.07)	0.235		
Fasting blood sugar (by every 100 mg/dL)	1.35 (0.74-2.45)	0.340		
Hemoglobin (by every 1 g/dL)	0.93 (0.67-1.31)	0.683		
Platelet counts (by every 10⁴/μL)	0.90 (0.82-0.99)	0.037	0.92 (0.78-1.08)	0.296
HCV load (by every 100 KIU/mL)	1.00 (1.00-1.00)	0.688		
Core 70 & 91 double mutation				
Wild	1		1	
Mutant	3.92 (1.14-13.5)	0.030	11.1 (1.40-88.7)	0.023
ISDR				
Nonwildtype	1			
Wildtype	1.38 (0.13-3.61)	0.513		
IL28B genotype				
Major allele†	1		1	
Minor allele‡	3.91 (1.52-10.0)	0.005	1.53 (0.20-11.9)	0.684
Hepatic gene expression (by every 0.1 copy/int. control)				
RIG-I	1.28 (1.10-1.50)	0.002	1.53 (1.07-2.22)	0.021
MDA5	1.53 (1.12-2.00)	0.001		
LGP2	1.34 (1.04-1.74)	0.026		
IPS-1	0.90 (0.78-1.04)	0.143		
RNF125	0.93 (0.83-1.04)	0.204		
ISG15	1.37 (1.16-1.62)	<0.001	1.28 (1.04-1.58)	0.021
USP18	1.67 (1.27-2.20)	<0.001		
IFNλ	1.02 (0.99-1.05)	0.170		
RIG-I/IPS-1 ratio (by every 0.1)	1.21 (1.07-1.36)	0.002		

Risk ratios for nonvirological response were calculated by the logistic regression analysis. BMI, body mass index; AST, aspartate aminotransferase; ALT, alanine aminotransferase; γ-GTP, gamma-glutamyl transpeptidase; HCV, hepatitis C virus; ISDR, IFN sensitivity determining region.
*Multivariate analysis was performed with factors significantly associated with nonvirological response by univariate analysis except for *MDA5, LGP2, USP18*, and *RIG-I/IPS-1* ratio, which were significantly correlated with *RIG-I* and *ISG15*.
†rs8099917 TT and rs12979860 CC.
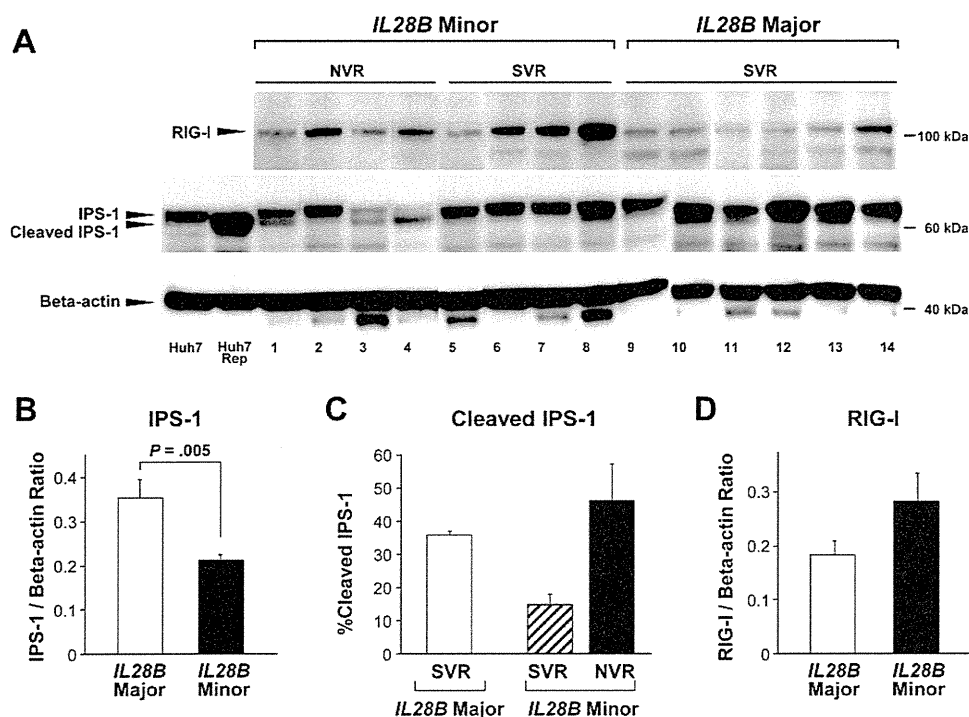‡rs8099917 TG and rs12979860 CT.

Fig. 5. (A) Western blotting for IPS-1 and RIG-I protein expression levels. Eight lanes contain samples from *IL28B* minor patients (lanes 1-8) and six lanes contain samples from *IL28B* major patients (lanes 9-14). Four lanes contain samples from nonvirological responders (NVR, lanes 1-4) and 10 lanes contain samples from sustained virological responders (SVR, lanes 5-14). Specific bands for RIG-I, full-length IPS-1, cleaved IPS-1, and β-actin are indicated by arrows. Naive Huh7 cells were used for a positive control for full-length IPS-1 (lane Huh7), and cells transfected with HCV-1b subgenomic replicon (Reference #20) were used for a positive control for cleaved IPS-1 (lane Huh7 Rep). (B) Total IPS-1 protein expression levels normalized to β-actin according to *IL28B* genotype. Error bars indicate standard error. *P*-value was determined by Mann-Whitney *U* test. (C) Percentage of cleaved IPS-1 products in total IPS-1 protein according to treatment responses stratified by *IL28B* genotype. Error bars indicate standard error. (D) RIG-I protein expression levels normalized to β-actin according to *IL28B* genotype. Error bars indicate standard error.

expression, total hepatic IPS-1 protein expression was significantly lower in *IL28B* minor patients than in *IL28B* major patients (Fig. 5B). With regard to *IL28B* minor patients, the percentage of cleaved IPS-1 protein in total IPS-1 in SVR was lower than that in NVR (Fig. 5C). In contrast to IPS-1 protein expression, hepatic RIG-I protein expression was higher in *IL28B* minor patients than that in *IL28B* major patients (Fig. 5D).

Discussion

In the present study we found that the baseline expression levels of intrahepatic viral sensors and related regulatory molecules were significantly associated with the genetic variation of *IL28B* and final virological outcome in CH-C patients treated with PEG-IFNα/RBV combination therapy. Although the relationship between the *IL28B* minor allele and NVR in PEG-IFNα/RBV combination therapy is evident, mechanisms responsible for this association remain unknown. *In vitro* studies have suggested that cytoplasmic viral sensors, such as RIG-I and MDA5, play a

pivotal role in the regulation of IFN production and augment IFN production through an amplification circuit.[7,8] Our results indicate that expressions of *RIG-I* and *MDA5* and a related amplification system may be up-regulated by endogenous IFN at a higher baseline level in *IL28B* minor patients. However, HCV elimination by subsequent exogenous IFN is insufficient in these patients, as reported,[19] suggesting that *IL28B* minor patients may have adopted a different equilibrium in their innate immune response to HCV. Our data are further supported by recent reports of an association between intrahepatic levels of IFN-stimulated gene expression and PEG-IFNα/RBV response as well as with *IL28B* genotype.[21-23]

In contrast to cytoplasmic viral sensor (*RIG-I*, *MDA5*, and *LGP2*) and modulator (*ISG15* and *USP18*) expression, the adaptor molecule (*IPS-1*) expression was significantly lower in *IL28B* minor patients. Moreover, western blotting further confirmed IPS-1 protein downregulation in *IL28B* minor patients by revealing decreased protein levels. Because IPS-1 is one of the main target molecules of HCV evasion,[9,18]

transcriptional and translational *IPS-1* expression are probably suppressed by HCV with resistant phenotype, which may be more adaptive in *IL28B* minor patients than in *IL28B* major patients. When we analyzed the proportion of full-length or cleaved IPS-1 to the total IPS-1 protein in a subgroup of *IL28B* minor patients, cleaved IPS-1 product was less dominant in SVR than in NVR, whereas uncleaved full-length IPS-1 protein was more dominant in SVR than in NVR. Therefore, the ability of HCV to evade host innate immunity by cleaving IPS-1 protein and/or host capability of protection from IPS-1 cleavage is probably responsible for the variable treatment responses in *IL28B* minor patients.

Our results indicated a close association between *IL28B* minor patients with higher γ-GTP level and higher frequency of HCV core double mutants, which are known factors for NVR. In contrast, no significant association was observed between *IL28B* genotype and age, gender, or liver fibrosis, which are also known to be unfavorable factors for virological response to PEG-IFNα/RBV. Therefore, certain factors other than the *IL28B* genotype may independently influence virological response. To elucidate whether gene expression involving innate immunity independently associates with a virological response from the *IL28B* genotype, we performed further analysis in a subgroup and conducted a multivariate regression and ROC analyses. Our multivariate and ROC analyses demonstrate that higher expressions of *RIG-I* and *ISG15* as well as a higher ratio of *RIG-I/IPS-1* are independently associated with NVR, and quantification of these values is more useful in predicting final virological response to PEG-IFNα/RBV than determination of *IL28B* genotype in each individual patients. However, the SVR rates in our patients were similar among *IL28B* genotypes, which suggests more SVR patients with the *IL28B* minor allele were included in the present study than those in the general CH-C population. Hence, our data did not necessarily exclude the possibility of the *IL28B* genotype in predicting NVR, although our multivariate analysis could not identify the *IL28B* minor allele as an independent factor for NVR. Interestingly, an association between *IL28B* genotype and expressions of *RIG-I* and *ISG15* as well as *RIG-I/IPS-1* expression ratio is still observed even in patients with the same subgroup of virological response (Fig. 3).

In the present study, although hepatic *IFNλ* expression was observed to be higher in *IL28B* minor and NVR patients, it was not statistically significant. Because *IL28B* shares 98.2% homology with *IL28A*, our primer could not distinguish the expression of

IL28B from that of *IL28A*, and moreover, we could not specify which cell expresses *IFNλ* (i.e., hepatocytes or other immune cells that have infiltrated the liver). Therefore, the precise mechanisms underlying *IL28B* variation and expression of *IFNλ* in relation to treatment response need further clarification by specifying type of IFNλ and uncovering the producing cells.

In the present study we included genotype 1b patients because it is imperative to designate a virologically homogenous patient group to associate individual treatment responses with different gene expression profiles that direct innate immune responses. We have reported that the *RIG-I/IPS-1* ratio was significantly higher in NVR with HCV genotype 2.[19] However, our preliminary results indicated that baseline hepatic *RIG-I* and *ISG15* expression and the *RIG-I/IPS-1* expression ratio is not significantly different among *IL28B* genotypes in patients infected with genotype 2 (Supporting Figure). This may be related to the rarity of NVR with HCV genotype 2 and the lower effect of *IL28B* genotype on virological responses in patients infected with HCV genotype 2.[24] The association among treatment responses in all genotypes, the different status of innate immune responses, and *IL28B* genotype needs to be examined further.

Differences in allele frequency for *IL28B* SNPs among the population groups has been reported. The frequency of *IL28B* major allele among patients with Asian ancestry is higher than that among patients with European and African ancestry.[25] Because *IL28B* polymorphism strongly influences treatment responses within each population group,[5] our data obtained from Japanese patients can be applied to other population groups. However, the rate of SVR having African ancestry was lower than that having European ancestry within the same *IL28B* genotype.[5] Hence, further study is required to clarify whether this difference among the population groups with the same *IL28B* genotype could be explained by differences in expression of genes involved in innate immunity.

In a recent report, an SVR rate of telaprevir with PEG-IFNα/RBV was only 27.6% in *IL28B* minor patients.[26] Because new anti-HCV therapy should still contain PEG-IFNα/RBV as a platform for the therapy, our findings regarding innate immunity in addressing the mechanism of virological response and predicting NVR remain important in this new era of directly acting anti-HCV agents, such as telaprevir and boceprevir.

In conclusion, this clinical study in humans demonstrates the potential relevance of the molecules involved in innate immunity to the genetic variation

of *IL28B* and clinical response to PEG-IFNα/RBV. Both the *IL28B* minor allele and higher expressions of *RIG-I* and *ISG15* as well as higher *RIG-I/IPS-1* ratio are independently associated with NVR. Innate immune responses in *IL28B* minor patients may have adapted to a different equilibrium compared with that in *IL28B* major patients. Our data will advance both understanding of the pathogenesis of HCV resistance and the development of new antiviral therapy targeted toward the innate immune system.

References

1. Kiyosawa K, Sodeyama T, Tanaka E, Gibo Y, Yoshizawa K, Nakano Y, et al. Interrelationship of blood transfusion, non-A, non-B hepatitis and hepatocellular carcinoma: analysis by detection of antibody to hepatitis C virus. HEPATOLOGY 1990;12:671-675.
2. Zeuzem S, Pawlotsky JM, Lukasiewicz E, von Wagner M, Goulis I, Lurie Y, et al. DITTO-HCV Study Group. International, multicenter, randomized, controlled study comparing dynamically individualized versus standard treatment in patients with chronic hepatitis C. J Hepatol 2005;43:250-257.
3. Tanaka Y, Nishida N, Sugiyama M, Kurosaki M, Matsuura K, Sakamoto N, et al. Genome-wide association of IL28B with response to pegylated IFN-alpha and ribavirin therapy for chronic hepatitis C. Nat Genet 2009;10:1105-1109.
4. Suppiah V, Moldovan M, Ahlenstiel G, Berg T, Weltman M, Abate ML, et al. IL28B is associated with response to chronic hepatitis C IFN-alpha and ribavirin therapy. Nat Genet 2009;10:1100-1104.
5. Ge D, Fellay J, Thompson AJ, Simon JS, Shianna KV, Urban TJ, et al. Genetic variation in IL28B predicts hepatitis C treatment-induced viral clearance. Nature 2009;461:399-401.
6. Biron CA. Initial and innate responses to viral infections—pattern setting in immunity or disease. Curr Opin Microbiol 1999;2:374-381.
7. Yoneyama M, Kikuchi M, Natsukawa T, Shinobu N, Imaizumi T, Miyagishi M, et al. The RNA helicase RIG-I has an essential function in double-stranded RNA-induced innate antiviral responses. Nat Immunol 2004;5:730-737.
8. Yoneyama M, Kikuchi M, Matsumoto K, Imaizumi T, Miyagishi M, Taira K, et al. Shared and unique functions of the DExD/H-box helicases RIG-I, MDA5, and LGP2 in antiviral innate immunity. J Immunol 2005;175:2851-2858.
9. Meylan E, Curran J, Hofmann K, Moradpour D, Binder M, Bartenschlager R, et al. Cardif is an adaptor protein in the RIG-I antiviral pathway and is targeted by hepatitis C virus. Nature 2005;437:1167-1172.
10. Kawai T, Takahashi K, Sato S, Coban C, Kumar H, Kato H, et al. IPS-1, an adaptor triggering RIG-I- and Mda5-mediated type I interferon induction. Nat Immunol 2005;6:981-988.
11. Seth RB, Sun L, Ea CK, Chen ZJ. Identification and characterization of MAVS, a mitochondrial antiviral signaling protein that activates NF-kappaB and IRF 3. Cell 2005;122:669-682.
12. Xu LG, Wang YY, Han KJ, Li LY, Zhai Z, Shu HB. VISA is an adapter protein required for virus-triggered IFN-beta signaling. Mol Cell 2005;19:727-740.
13. Rothenfusser S, Goutagny N, DiPerna G, Gong M, Monks BG, Schoenemeyer A, et al. The RNA helicase Lgp2 inhibits TLR-independent sensing of viral replication by retinoic acid-inducible gene-I. J Immunol 2005;175:5260-5268.
14. Arimoto K, Takahashi H, Hishiki T, Konishi H, Fujita T, Shimotohno K. Negative regulation of the RIG-I signaling by the ubiquitin ligase RNF125. Proc Natl Acad Sci U S A 2007;104:7500-7505.
15. Zhao C, Denison C, Huibregtse JM, Gygi S, Krug RM. Human ISG15 conjugation targets both IFN-induced and constitutively expressed proteins functioning in diverse cellular pathways. Proc Natl Acad Sci U S A 2005;102:10200-10205.
16. Schwer H, Liu LQ, Zhou L, Little MT, Pan Z, Hetherington CJ, et al. Cloning and characterization of a novel human ubiquitin-specific protease, a homologue of murine UBP43 (Usp18). Genomics 2000;65:44-52.
17. Malakhov MP, Malakhova OA, Kim KI, Ritchie KJ, Zhang DE. UBP43 (USP18) specifically removes ISG15 from conjugated proteins. J Biol Chem 2002;277:9976-9981.
18. Li XD, Sun L, Seth RB, Pineda G, Chen ZJ. Hepatitis C virus protease NS3/4A cleaves mitochondrial antiviral signaling protein off the mitochondria to evade innate immunity. Proc Natl Acad Sci U S A 2005;102:17717-17722.
19. Asahina Y, Izumi N, Hirayama I, Tanaka T, Sato M, Yasui Y, et al. Potential relevance of cytoplasmic viral sensors and related regulators involving innate immunity in antiviral response. Gastroenterology 2008;134:1396-1405.
20. Tanabe Y, Sakamoto N, Enomoto N, Kurosaki M, Ueda E, Maekawa S, et al. Synergistic inhibition of intracellular hepatitis C virus replication by combination of ribavirin and interferon-alpha. J Infect Dis 2004;189:1129-1139.
21. Honda M, Sakai A, Yamashita T, Nakamoto Y, Mizukoshi E, Sakai Y, et al. Hepatic ISG expression is associated with genetic variation in interleukin 28B and the outcome of IFN therapy for chronic hepatitis C. Gastroenterology 2010;139:499-509.
22. Urban TJ, Thompson AJ, Bradric SS, Fellay J, Schuppan D, Cronin KD, et al. IL28B genotype is associated with differential expression of intrahepatic interferon-stimulated genes in patients with chronic hepatitis C. HEPATOLOGY 2010;52:1888-1896.
23. Dill MT, Duong FHT, Vogt JE, Bibert S, Bochud PY, Terracciano L, et al. Interferon-induced gene expression is a stronger predictor of treatment response than IL28B genotype in patients with hepatitis C. Gastroenterology 2011;140:1021-1031.
24. Yu ML, Huang CF, Huang JF, Chang NC, Yang JF, Lin ZY, et al. Role of interleukin-28B polymorphism in the treatment of hepatitis C virus genotype 2 infection in Asian patients. HEPATOLOGY 2011;53:7-13.
25. Thomas DL, Thio CL, Martin MP, Qi Y, Ge D, O'hUigin C, Kidd J, et al. Genetic variation in IL28B and spontaneous clearance of hepatitis C virus. Nature 2009;461:798-802.
26. Akuta N, Suzuki F, Hirakawa M, Kawamura Y, Yatsuji H, Sezaki H, et al. Amino acid substitution in hepatitis C virus core region and genetic variation near the interleukin 28B gene predict viral response to teraprevir with pegIFN and ribavirin. HEPATOLOGY 2010;52:421-429.

Wnt5a Signaling Mediates Biliary Differentiation of Fetal Hepatic Stem/Progenitor Cells

Kei Kiyohashi[1*], Sei Kakinuma[1,2*], Akihide Kamiya[3,7], Naoya Sakamoto[1,4], Sayuri

Nitta[1], Hideto Yamanaka[1], Kouhei Yoshino[1], Junko Fijuki[1], Miyako Murakawa[1], Akiko

Kusano-Kitazume[1], Hiromichi Shimizu[1], Ryuichi Okamoto[1], Seishin Azuma[1], Mina

Nakagawa[1], Yasuhiro Asahina[1,2], Naoki Tanimizu[5], Akira Kikuchi[6], Hiromitsu

Nakauchi[3], and Mamoru Watanabe[1].

1 Department of Gastroenterology and Hepatology, Tokyo Medical and Dental

University, Tokyo, Japan

2 Department for Hepatitis Control, Tokyo Medical and Dental University, Tokyo,

Japan

3 Division of Stem Cell Therapy, Institute of Medical Science, The University of Tokyo,

Tokyo, Japan

4 Department of Gastroenterology, Hokkaido University, Sapporo, Japan

5 Department of Tissue Development and Regeneration, School of Medicine, Sapporo

Medical University, Sapporo, Japan

2

6 Department of Molecular Biology and Biochemistry, Graduate School of Medicine,

Osaka University, Osaka, Japan

7 Institute of Innovative Science and Technology, Tokai University, Isehara, Japan

* These authors contributed equally to this study.

Key Words:

Contact information

Address reprint requests to: Sei Kakinuma, M.D., Ph.D., and Mamoru Watanabe, M.D.,

Ph.D., Department of Gastroenterology and Hepatology, Tokyo Medical and Dental

University, 1-5-45 Yushima, Bunkyo-ku, Tokyo, 1138519 Japan.   Tel:

+81-3-3813-6111.   Fax: +81-3-5803-0268.   E-mail: skakinuma.gast@tmd.ac.jp (S.

Kakinuma) and mamoru.gast@tmd.ac.jp (M. Watanabe)

Abbreviations:

Ab, antibody; ALB, albumin; CaMKII, calcium/calmodulin-dependent kinase II; CK,

cytokeratin; CPS, carbamoyl phosphate synthetase; DAPI;

3

4',6-diamidino-2-phenylindole; DMSO, dimethyl sulfoxide; E, embryonic day; EGF,

Epidermal growth factor; FCS, fetal calf serum; HGF, hepatocyte growth factor; HNF,

hepatic nuclear factor; MRP, multidrug resistance-associated protein; P, postnatal day;

PCNA, proliferating cell nuclear antigen; PFA, paraformaldehyde; PKC, Protein kinase

C; RT, reverse transcriptase; TCF, T-cell factor; TAT, tyrosine aminotransferase; TGF,

transforming growth factor; TO, tryptophan-2,3-dioxygenase.

Potential conflict of interest.   Nothing to report.

4

Abstract

The molecular mechanisms regulating differentiation of fetal hepatic stem/progenitor cells, called *hepatoblasts*, which play pivotal roles in liver development, remain obscure.

Wnt signaling pathways regulate the development and differentiation of stem cells in various organs.   While a β-catenin-independent non-canonical Wnt pathway is essential for cell adhesion and polarity, the physiological functions of non-canonical Wnt pathways in liver development are unknown.   Here we describe a functional role for Wnt5a, a non-canonical Wnt ligand, in the differentiation of mouse hepatoblasts.

Wnt5a was expressed in mesenchymal cells and other cells of wild-type mid-gestational fetal liver.   We analyzed fetal liver phenotypes in Wnt5a-deficient mice using a combination of histological and molecular techniques.   Expression levels of Sox9 and the number of HNF1β-positive HNF4α-negative biliary precursor cells were significantly higher in Wnt5a-deficient liver relative to wild-type liver.   In Wnt5a-deficient fetal liver, *in vivo* formation of primitive bile ductal structures was significantly enhanced relative to wild-type littermates.   We also investigated the function of Wnt5a protein and downstream signaling molecules using a three-dimensional culture system that included primary hepatoblasts or a hepatic progenitor cell line.   *In vitro* differentiation assays showed that Wnt5a retarded the formation of bile duct-like structures in hepatoblasts, leading instead to hepatic

5

maturation of such cells.   While Wnt5a signaling increased steady-state levels of

phosphorylated Calcium/calmodulin-dependent protein kinase II (CaMKII) in fetal liver,

inhibition of CaMKII activity resulted in the formation of significantly more and

larger-sized bile duct-like structures *in vitro* compared with those in

vehicle-supplemented controls.

Conclusions: We demonstrate that Wnt5a-mediated signaling in fetal hepatic

stem/progenitor cells suppresses biliary differentiation. We also suggest that activation

of CaMKII by Wnt5a signaling suppresses biliary differentiation.

6

Introduction

Hepatic stem cells are multipotent stem cells located within ductal plates in fetal and neonatal livers, and canals of Hering in pediatric and adult livers.[1] The extrahepatic stem cell niches are peribiliary glands within the bile ducts in humans.[2] Hepatic stem/progenitor cells, called hepatoblasts in fetal liver, proliferate actively and give rise to hepatocytes and cholangiocytes.[3, 4] Lineage commitment of such cells can be traced by several cell surface markers, including NCAM, ICAM-1, and EpCAM, in humans.[1, 5] While our group[6] and others[7] demonstrated roles for transcription factors regulating the biliary differentiation of hepatic stem/progenitor cells, the molecular mechanisms behind these events have yet to be fully elucidated.

The Wnt-family secreted ligands and the corresponding Frizzled-family cell surface receptors play a crucial role in the differentiation, proliferation, and self-renewal of stem cells in various organs.[8] Wnt signaling pathways involve interactions between a complex set of molecular cognates that includes 19 different Wnt ligands and 10 Frizzled (Fzd) receptors in humans and mice (reviewed at http://www.stanford.edu/~rnusse/wntwindow.html). Upon binding to Fzd receptors on the surface of a target cell, Wnt proteins activate one of two classes of downstream pathways distinguishable by their dependency on β-catenin. Examples of canonical β-catenin-dependent pathways include β-catenin-dependent activation of T-cell factor

7

(TCF) by either Wnt1 or Wnt3.[8] In contrast, Wnt4 and Wnt5a activate non-canonical

β-catenin independent pathways that include downstream molecules such as

Calcium/calmodulin-dependent protein kinase II (CaMKII), Rho-kinase, Rac1,

Calcineurin, and Protein kinase C (PKC).[9]

In liver development, β-catenin is known to regulate the maturation, expansion,

and survival of hepatoblasts, and its deletion results in increased apoptosis of

hepatoblasts in mid-gestational fetal livers.[10] While the function of non-canonical Wnt

signaling in liver development is currently unknown, β-catenin-independent Wnt

pathways have been shown to function predominantly as regulators of cell polarity and

mobility in other organs.[9] In systemic Wnt5a-deficient (KO) mice, the size of caudal

structures, lung morphogenesis, and intestinal elongation are also abnormal.[11-13]

Recent reports demonstrate that Wnt5a regulates hematopoietic, mesenchymal,

and neural stem cell functions.[14-16] Wnt5a has been shown to increase the repopulation

of short- and long-term hematopoietic stem cells by maintaining these cells in a

quiescent G0 state.[14] Wnt5a maintains mesenchymal stem cells and promotes

osteoblastogenesis in preference to adipogenesis in bone marrow,[15] and also improves

the differentiation and functional integration of stem cell-derived dopamine neurons.[16]

In healthy adult mouse liver, Wnt5a is expressed in mature hepatocytes and

cholangiocytes.[17] Nonetheless, the physiological functions of Wnt5a and the signaling

8

cascades that it initiates during liver development and in hepatic stem/progenitor cells

are unknown.

In this study, we investigated the function of Wnt5a and its downstream targets in

the development of murine fetal hepatic stem/progenitor cells. Analysis on Wnt5a KO

mice demonstrated that loss of Wnt5a abnormally promotes the formation of bile ductal

structures in fetal liver *in vivo*. Wnt5a-supplementation not only retarded the formation

of bile-duct like structures, but also promoted hepatic maturation of hepatic

stem/progenitor cells *in vitro*. CaMKII activity, which showed Wnt5a-dependence in

fetal liver, suppressed the formation of bile-duct like structures. These data indicate that

Wnt5a-mediated CaMKII signaling plays an essential role in the differentiation of

murine fetal hepatic stem/progenitor cells.

9

Materials and Methods

Animals

Systemic Wnt5a KO mice in C57BL/6 background were originally generated by

Yamaguchi et al.[11] Wnt5a KO mice and wild type (WT) littermates were produced by

crossbreeding Wnt5a heterozygous mice. All animals were treated based on the

guidelines of the Institute of Medical Science, University of Tokyo and those of Tokyo

Medical and Dental University.

In vitro bile duct-like differentiation assay of primary hepatoblasts

Bile duct-like differentiation assays were performed as previously described[6] with

some modifications.   Fetal hepatic cells of E14.5 liver were dissociated with

collagenase[4] and Dlk^{+} cells were isolated from the resulting population using a

magnetic cell sorter (MACS; Miltenyi Biotec, Bergisch Gladbach, Germany) and then

cultured in collagen gel (Nitta Gelatin, Osaka, Japan).   After 30 minutes of incubation

at 37°C on basal-layer collagen, 1 or 2×10^4 cells were suspended in 1 ml DMEM/F12,

mixed with 1 ml collagen gel solution, and plated onto basal-layer collagen in 6-well

culture dishes.   Plated cells were cultured for 7 days with an additional 2 ml DMEM

supplemented with 10% fetal calf serum (FCS, Sigma, St. Louis, MO),

1×insulin/transferrin/selenium, 20 ng/ml epidermal growth factor (EGF, PeproTech,

10

Rocky Hill, NJ), 20 ng/ml hepatocyte growth factor (HGF, PeproTech) and 25 ng/ml

tumor necrosis factor α (PeproTech).

In vitro bile duct-like differentiation assay of hepatic progenitor cell line

The HPPL liver progenitor cell line has been reported to exhibit characteristics of

differentiated cholangiocytes in three-dimensional culture.[18, 19] As in the previous report,

we maintained HPPL cells in DMEM/F-12 containing 10% FCS, 1 ×

insulin/transferrin/selenium, 10 mM nicotinamide, 10^{-7} M Dex, and 5 ng/ml HGF and

EGF and suspended cells in a mixture of type I collagen and Engelbreth-Holm-Swarm

sarcoma gel (EHS gel, Becton Dickinson, Bedford, MA) at a density of 4×10^4 cells/ml.

Cell suspension was added to each cell culture insert (Millipore, Billerica, MA) and

after incubation at 37°C for 2 h, 500 μl of DMEM/F-12 with growth factors was added

above and below the insert and the cells were cultured for seven days.   To test the

effects of inhibitors of CaMKII, Rho-kinase, Rac1, Calcineurin, and PKC on HPPL

differentiation, KN93, KN92, KN62, Y-27632, NSC23766, Cyclosporin A, and Go6976

(see *Materials* in Supplementary file) were added individually to the culture medium

when each three-dimensional culture was initiated. Independent analyses were

performed in triplicate and 5 fields were randomly selected for counting the cysts that

indicate bile duct-like differentiation of cells.

11

In vitro hepatic maturation assay of primary hepatoblasts

To induce hepatic differentiation, primary hepatoblasts from WT E14.5 mice

were cultured as previously described.[6] Briefly, 2.5×10^5 MACS-isolated Dlk$^+$ cells

were cultured in DMEM supplemented with 10% FCS, 2 mM L-glutamine, $1 \times$

non-essential amino acid, 100 U/ml penicillin, 100 µg/ml streptomycin, 10^{-7} M Dex

in each well of a 6-well gelatin-coated dish.   After 5 days, the resulting cells were

supplemented with medium containing 20% EHS gel for an additional 2 days prior

to analysis.

Materials and methods providing details of materials, cell isolation,

Hematoxylin-eosin (HE) staining, RT-PCR analysis, immunostaining, immunoblot

analysis, Wnt5a-blocking experiments, microarray analysis, and statistics procedures

are described in the Supplementary file.

12

Results

Expressions of Wnt5a and Frizzled receptors during liver development

We first analyzed *Wnt5a* expression during liver development using quantitative

RT-PCR. *Wnt5a* expression was detected in fetal and neonatal livers of WT mice and

showed a gradual increase during liver development (Fig. 1A). To investigate Wnt5a

expression in mid-gestational fetal liver, we purified the fractions of hepatoblasts,

mesenchymal cells, mesothelial cells, endothelial cells, and hematopoietic cells from

E14.5 liver using FACS. Quantitative RT-PCR analysis indicated that *Wnt5a* was

expressed in hepatoblasts, mesenchymal cells, mesothelial cells, endothelial cells, and

hematopoietic cells. The expression level of Wnt5a was significantly higher in

mesenchymal cells than in hepatoblasts and other types of cells in mid-gestational fetal

liver (Fig. 1B).   Frizzled is a family of cell surface receptors for Wnt ligands. Adult

hepatocytes from 12-week-old mice served as the control. RT-PCR analysis of E14.5

hepatoblasts resulted in detection of 9 of 10 Fzd receptors (all except *Fzd9*), whereas

E14.5 hematopoietic cells expressed 9 of 10 Fzd receptors (all except *Fzd2*, Fig. 1C and

supplementary Fig. 1).

Loss of Wnt5a promotes the formation of bile duct in fetal liver

Since one of the reported phenotypes of systemic Wnt5a KO mice was postpartum

13

death[11], we investigated the function of Wnt5a in liver development using mid- to

late-gestational fetuses. We determined that although average liver weight in Wnt5a KO

E18.5 fetal mice was significantly lower than in WT littermates, the average ratio of

liver:body weight in the KO mice was not significantly different from the ratio in WT

mice (supplementary Fig. 2).

Histological analysis of E18.5 livers showed that the number of luminal spaces

around the portal vein, which we interpret to be primitive bile ducts, was greater in

Wnt5a KO mice than in WT mice (Fig. 2A). To further investigate these changes in

bile duct development, expression of *Sox9* (a representative transcriptional factor

expressed in biliary precursor cells)[20] was analyzed. Expression levels of *Sox9* were

significantly higher in Wnt5a KO E16.5 fetal livers relative to WT livers (Fig. 2B). The

Notch pathway plays an essential role in the morphogenesis of bile duct structures.[21]

Expression levels of *Notch1*, *Notch2*, and *Jagged1* were significantly higher in Wnt5a

KO E16.5 fetal livers relative to WT livers (supplementary Fig. 3A). Numbers of Hes1^{+}

cells in E18.5 livers were significantly greater in Wnt5a KO mice than in WT mice

(supplementary Fig. 3B). Expression levels of *Cyclin D1* and *c-Myc* (target transcripts

of canonical β-catenin-dependent Wnt pathway) in Wnt5a KO livers were equal to those

in WT livers (supplementary Fig. 4A). We tried to assess the protein level of Sox9,

however, immunostaining analysis of Sox9 did not work well probably due to technical

14

problems (data not shown).

During normal liver development, hepatoblasts located around the portal vein develop as hepatocyte nuclear factor (HNF)1β⁺HNF4α⁻ biliary precursor cells.[22] In normal E16.5 fetal livers, monolayer rings of biliary precursor cells, termed ductal plates, can be detected.[23] Two-day older WT E18.5-stage fetal livers contained primitive ductal structures (PDS) consisting of multiple HNF1β⁺CK19⁺-cell lumina (Fig. 2C).

Immunohistological analysis revealed that numbers of HNF1β⁺HNF4α⁻ biliary precursor cells in E16.5 livers (Fig. 2D) and in PDS formed by these cells in E18.5 livers (Fig. 2E) were significantly higher in Wnt5a KO mice relative to WT mice. Double staining of CK19 and entactin (a component of basement membrane) confirmed that the number of PDS formed by CK19⁺ cells was also significantly higher in E18.5 Wnt5a KO liver relative to the WT (Fig. 2F). These results demonstrate clearly that loss of Wnt5a excessively promotes the formation of bile ducts in fetal liver.

Expression analysis of fetal livers in Wnt5a KO mice

Expression of genes coincident with hepatic maturation was also analyzed in Wnt5a KO fetal livers using quantitative RT-PCR. In E16.5 fetal livers, ALB and HNF4α mRNA levels were nearly equal between WT and Wnt5a KO mice. Similarly, we observed no significant differences between WT and Wnt5a KO E18.5 fetal livers

15

with regard to copy numbers of tyrosine aminotransferase (TAT), carbamoyl phosphate

synthetase 1 (CPS1), glucose-6-phosphatase (G6Pase), or HNF4α mRNAs

(supplementary Figs. 5A and B). These data suggest that the maturation of hepatoblasts

to hepatocytes is not impaired in Wnt5a KO mice.

Proliferation of fetal liver cells in Wnt5a KO mice was analyzed by immunoblot

and immunostaining.   Immunoblot analysis revealed that PCNA production in Wnt5a

KO livers was almost equal to that in WT livers (supplementary Fig. 4B). Numbers of

CK19$^+$PCNA$^+$ cells in E18.5 were almost equal to those in WT livers (supplementary

Fig. 4C).   Changes in gene expression in Wnt5a KO livers were analyzed using cDNA

microarray analysis (supplementary Fig. 5C and supplementary Table 5).   Cluster

analysis revealed that several molecules associated with amino acid metabolism and cell

migration were upregulated or downregulated in Wnt5a KO fetal livers compared with

those in WT livers.

Wnt5a retards formation of bile duct-like structures from primary hepatoblasts

In collagen gel-embedding culture, mouse primary hepatoblasts differentiate into

bile duct-like branching structures, coincident with the expression of biliary

cell-specific genes such as CK19 (Fig. 3A, left panel).[6] To investigate the effects of

Wnt5a on differentiation of hepatoblasts into biliary cells *in vitro*, we cultured primary

16

hepatoblasts derived from E14.5 WT fetal livers, and assessed the formation of bile

duct-like branching structures.

We observed that cells in cultures derived from E14.5 WT fetal liver formed

approximately 10 colonies (consisting of >100 cells in large branching structures) per

1×10^4 cells (Fig. 3A, right panel); colonies with medium (50-99 cells) or small (10-49

cells) branching structures also were noted. In cultures supplemented with Wnt5a, there

were significant decreases in the average number colonies with large- and

medium-sized branching structures relative to vehicle-only controls.

Wnt5a suppresses cyst formation derived from HPPL in three-dimensional culture

To assess the potential of hepatic stem/progenitor cells for bile-duct like luminal

formation, we used an HPPL three-dimensional culture system.[19] HPPL is established

from mouse E14 Dlk[+] hepatoblasts, and differentiates into hepatic and cholangiocytic

lineages.[18] In this system, HPPL cells form cysts that exhibit characteristics of

differentiated cholangiocytes producing CK19, E-cadherin, and other characteristic

markers.   We categorized HPPL-derived colonies into one of three classes: colonies

without clear lumina, small cysts (50-100 μm diameter with clear lumina), and large

cysts (>100 μm diameter with clear lumina).   As previously described,[19]

immunocytostaining of cultured cells showed that colonies without clear lumina